the FEBS Journal

Uth1 is a mitochondrial inner membrane protein dispensable for post-log-phase and rapamycin-induced mitophagy

Evelyn Welter[1,*], Marco Montino[1,*], Robert Reinhold[1,*], Petra Schlotterhose[1], Roswitha Krick[1], Jan Dudek[1], Peter Rehling[1,2] and Michael Thumm[1]

1 Department of Cellular Biochemistry, Georg-August University, Göttingen, Germany
2 Max-Planck Institute for Biophysical Chemistry, Göttingen, Germany

Keywords
Atg32; Atg33; macroautophagy; mitophagy; *Saccharomyces cerevisiae*; Uth1; Yme1

Correspondence
M. Thumm, Institute of Cellular Biochemistry, Georg-August University, Humboldtallee 23, D-37073 Göttingen, Germany
Fax: +49 551 39 5979
Tel: +49 551 39 5947
E-mail: mthumm@uni-goettingen.de
P. Rehling, Institute of Cellular Biochemistry, Georg-August University, Humboldtallee 23, D-37073 Göttingen and Max-Planck Institute for Biophysical Chemistry, D-37077 Göttingen, Germany
Fax: +49 551 39 5979
Tel: +49 551 39 5947
E-mail: peter.rehling@medizin.uni-goettingen.de

*These authors contributed equally to this paper

(Received 28 February 2013, revised 1 July 2013, accepted 19 July 2013)

doi:10.1111/febs.12468

Mitochondria are turned over by an autophagic process termed mitophagy. This process is considered to remove damaged, superfluous and aged organelles. However, little is known about how defective organelles are recognized, what types of damage induce turnover, and whether an identical set of factors contributes to degradation under different conditions. Here we systematically compared the mitophagy rate and requirement for mitophagy-specific proteins during post-log-phase and rapamycin-induced mitophagy. To specifically assess mitophagy of damaged mitochondria, we analyzed cells accumulating proteins prone to degradation due to lack of the mitochondrial AAA-protease Yme1. While autophagy 32 (Atg32) was required under all tested conditions, the function of Atg33 could be partially bypassed in post-log-phase and rapamycin-induced mitophagy. Unexpectedly, we found that Uth1 was dispensable for mitophagy. A re-evaluation of its mitochondrial localization revealed that Uth1 is a protein of the inner mitochondrial membrane that is targeted by a cleavable N-terminal pre-sequence. In agreement with our functional analyses, this finding excludes a role of Uth1 as a mitochondrial surface receptor.

Introduction

Macroautophagy is a starvation-induced bulk degradation pathway highly conserved among eukaryotes. In brief, cytosolic material is unselectively enclosed into autophagosomes. These double-membrane-layered vesicles form out of a crescent-shaped phagophore (isolation membrane) at the pre-autophagosomal structure/phagophore assembly site (PAS). They fuse with the vacuole and release a single-membraned

Abbreviations
Atg, autophagy; CMAC, 4-chloromethyl-7-aminocoumarin; FM4-64, *N*-(3-triethylammoniumpropyl)-4-(*p*-diethylaminophenylhexatrienyl) pyridinium dibromide; GFP, green fluorescent protein; mito-GFP, mitochondria-localized GFP-fusion protein; PAS, pre-autophagosomal structure/phagophore assembly site; ROS, reactive oxygen species.

autophagic body into the vacuole. Here the autophagic body is degraded together with its cargo for reuse of its building blocks [1–4].

Besides unselective macroautophagy a growing number of selective variants, especially for the uptake of bulky substrates such as protein aggregates, parts of organelles, invading bacteria and even parts of the nucleus, have been discovered. Among the more than 30 known autophagy (Atg) proteins a set of core proteins is essential for all subtypes while additional factors act as subtype-specific components linking individual autophagy pathways to the core machinery. One such selective pathway is mitophagy, which is responsible for removing superfluous or damaged mitochondria. It has gained increasing interest due to its important roles in development and disease [5–8].

During reticulocyte maturation mitochondria are degraded by mitophagy depending on the mitochondrial outer membrane protein NIX (BNIP3L), which serves as a mitophagy receptor [9–11]. Moreover, a non-canonical form of mitophagy was observed during erythroid maturation that is independent of the core autophagy proteins Atg5 and Atg7 [12]. Recent analysis of autosomal recessive forms of Parkinson's disease revealed a link to mitophagy as well [8]. Patients with mutations in genes coding for the outer mitochondrial membrane kinase PINK1 and the cytosolic E3 ubiquitin ligase Parkin have been identified. It has been suggested that mitochondrial damage leads to stabilization of PINK1, which then causes mitochondrial recruitment of Parkin [13,14]. Parkin mediates polyubiquitination via Lys27 and Lys63 of mitochondrial substrates [15]. Among the so far proposed substrates of Parkin are VDAC1 (voltage-dependent anion channel 1) and mitofusins (involved in mitochondrial fusion) [16–18]. Subsequent degradation of mitofusins dependent on the proteasome and the AAA+ ATPase p97 led to the hypothesis that this mechanism could result in the segregation of damaged mitochondrial fragments followed by their autophagic removal [19]. In line with this hypothesis specific starvation conditions led to downregulation of the mitochondrial fission protein Drp1. The resulting mitochondrial elongation resulted in reduced autophagic removal of mitochondria [20]. In yeast the role of mitochondrial fission and fusion during mitophagy is not fully understood; some studies reported a function of the mitochondrial fission protein Dnm1 (the yeast orthologue of Drp1), whereas another found it to be dispensable [21–23].

In *Saccharomyces cerevisiae* two genome-wide screens identified, in addition to the autophagic core machinery, Atg32 as a mitophagy-specific transmembrane protein of the mitochondrial outer membrane [21,24,25]. Typical for an autophagic cargo receptor, Atg32 interacts with Atg8 via a highly conserved W/YxxL/I motif in its cytosolic N-terminal region [24,25]. NIX has no yeast homologue, but similar to Atg32 it contains a W/YxxL/I motif, which binds to mammalian Atg8 homologues [10,11]. Atg32 further interacts with Atg11, an autophagy protein expected to act as a scaffold at the PAS during selective autophagy variants. This interaction is mediated by phosphorylation of Atg32 [26].

To induce mitophagy in yeast two conditions have been widely used: cells are either grown for extended times under respiratory conditions (post-log-phase mitophagy) or respiratory cells are shifted to a medium containing glucose but lacking nitrogen (starvation-induced mitophagy) [21,24,25,27–29]. Under both conditions superfluous mitochondria are removed, but during post-log-phase mitophagy also aged mitochondria might be targets of mitophagy. Interestingly, components such as Atg33 are specific for individual mitophagy-inducing conditions. Atg33 was reported to be essential for post-log-phase mitophagy, while its absence only partially affected starvation-induced mitophagy [21].

Mitochondria as the powerhouse of the cell are a major site of ATP production, but at the same time they generate reactive oxygen species (ROS). ROS can damage mitochondria and other cellular components. Mitochondrial damage implies the risk of enhanced ROS production and may even lead to induction of cell death by the release of pro-apoptotic proteins [30,31]. To prevent excessive ROS production by dysfunctional mitochondria, a tight mitochondrial quality control system is necessary [8,32]. Selective mitophagy of damaged mitochondria is expected as a means to protect cells from overshooting ROS production.

Uth1 is a member of the SUN (Sim1, Uth1, Nca3) family; these homologous proteins are related to a β-glucosidase of *Candida wickerhamii* and are involved in different cellular functions. Uth1 is localized to both the cell wall, from which it can be released with dithiothreitol, and the mitochondrial outer membrane. It affects mitochondrial biogenesis, cell wall biogenesis and life span [33–35]. *uth1*Δ cells are further resistant to H_2O_2 but sensitive to superoxide-radical-generating paraquat [36]. Uth1 was reported to be required for rapamycin-induced mitophagy but not for unselective macroautophagy [37]. A more detailed study suggested that Uth1 is involved in a selective type of mitophagy where mitochondria are engulfed without significant amounts of cytosol, while in the absence of Uth1 engulfment of mitochondria together with large portions of the cytosol still occurred [38]. The specificity of Uth1 for selective mitophagy and its proposed localization at the mitochondrial outer membrane prompted us

to speculate that it might have a receptor-like function, probably in concert with Atg32. Since the role of Uth1 in mitophagy has been questioned in other studies [24,25], we here addressed the requirement for mitochondrial mitophagy factors in post-log-phase and rapamycin-induced mitophagy. Our analyses show no essential role of Uth1 in mitophagy under these conditions. A primary sequence analysis of Uth1 revealed the presence of a predictable N-terminal mitochondrial targeting signal suggesting that the protein is transported across the inner membrane of mitochondria. In contrast to previous reports, we show that Uth1 is an inner mitochondrial membrane protein that is processed upon import in a membrane-potential-dependent manner. This argues against a role of Uth1 as an outer membrane mitophagy receptor.

Results

Requirement of mitophagy-specific proteins for post-log-phase mitophagy

To monitor mitophagy we generated a mitochondria-localized fusion protein (mito-GFP) consisting of the established model protein Su9-DHFR (the pre-sequence of *Neurospora crassa* subunit 9 of the F_1F_0 ATPase fused to mouse dihydrofolate reductase) fused to green fluorescent protein (GFP) and used this construct for degradation assays [25,39]. Mitochondria labeled with the mito-GFP fusion protein are transported to the vacuolar lumen via mitophagy, where their breakdown results in formation of a proteolysis-resistant GFP released from the mito-GFP fusion. Accordingly, the level of free GFP determined in western blots corresponds to the mitophagy rate. Previous studies induced mitophagy in lactate-grown cells (a) by extended growth in lactate medium up to 72 h (post-log-phase mitophagy) [25,27], (b) by shifting the cells to SD-(N), a nitrogen-free glucose-containing medium [27,38], or (c) by adding the TOR kinase inhibitor rapamycin [23,37]. Since the requirement of mitophagy-specific proteins, especially those of Uth1, under different inducing conditions are not fully understood, we systematically analyzed mitophagy in cells lacking Atg32, Atg33 or Uth1. In our hands shift of lactate-grown cells to SD-(N) medium did not induce robust mitophagy. Therefore, we focused our analyses on post-log and rapamycin-induced mitophagy. As expected, during post-log-phase mitophagy *atg32*Δ cells showed a complete block, comparable to cells deficient for the core autophagy protein Atg18 (Fig. 1A). While *atg33*Δ cells exhibited a reduced mitophagy rate, *uth1*Δ cells displayed no significant defect in mitophagy (Fig. 1A,B).

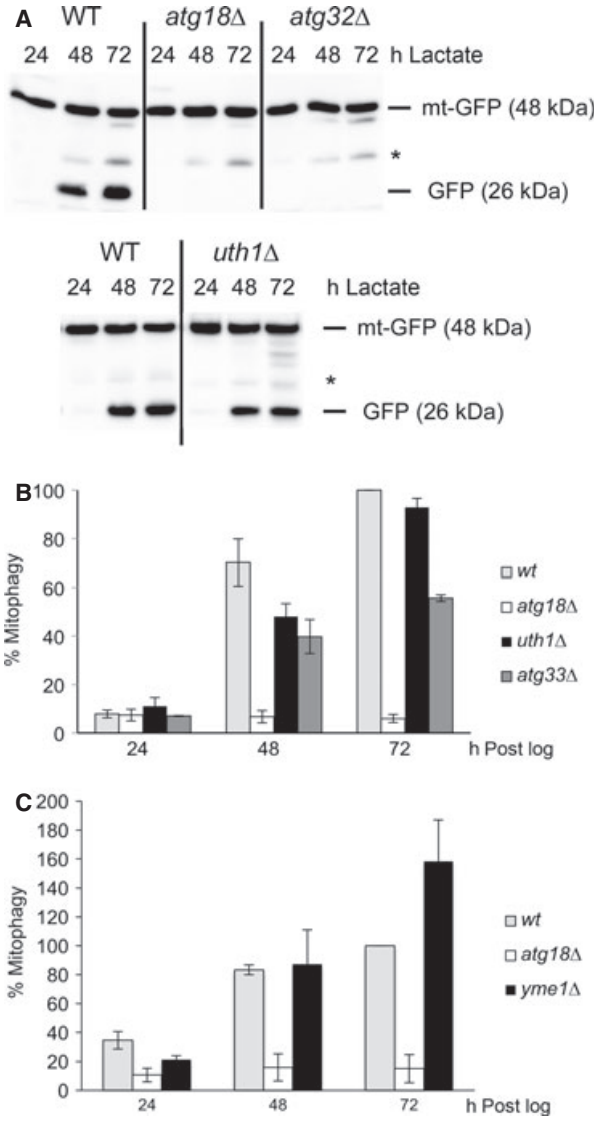

Fig. 1. Post-log-phase mitophagy. (A) The vacuolar breakdown of a GFP-fusion protein yields proteolysis-stable free GFP. Cells of the BY4742 background expressing Su9-DHFR (the pre-sequence of *N. crassa* subunit 9 of the F_1F_0 ATPase fused to mouse dihydrofolate reductase and GFP) were grown in selection medium with 2% lactate, and samples were taken and treated for western blot analysis as described in Experimental procedures. *cross-reacting material; WT, wild type. (B) The mitophagy rate was calculated by quantification of GFP signal intensities. The value of lactate-grown wild-type cells after 72 h was set to 100%. The standard error of the mean was calculated from at least three independent experiments. (C) WCG4α wild-type, *atg18*Δ and *yme1*Δ cells expressing mito-GFP (mt-GFP) were stationary grown in selection medium with 2% lactate; samples were taken after 24, 48 and 72 h and treated for western blotting. Mitophagy rate was calculated by quantification of GFP signal intensities. The value of lactate-grown wild-type cells after 72 h was set to 100%. The standard error of the mean is from at least three independent experiments.

To monitor unselective macroautophagy, we examined in parallel cells expressing Pgk1-GFP [40]. Similar to the mito-GFP assay, the level of GFP generated by autophagic degradation of the cytosolic marker protein Pgk1-GFP reflects the macroautophagic rate. In agreement with previous reports, unselective macroautophagy was concomitantly induced during post-log-phase mitophagy [27]. Consistent with its role as cargo receptor, Atg32 did not influence macroautophagy, and no significant macroautophagy defects were observed in *atg33*Δ or *uth1*Δ cells (not shown).

Besides external signaling, internal stimuli such as mitochondrial damage induce mitophagy. In the case of the pathology of Parkinson's disease quality control through mitophagy plays an important role [8]. Thus, we aimed to follow selective removal of damaged mitochondria in yeast under conditions that act at the level of the organelle. The mitochondrial uncoupler carbonyl cyanide *m*-chlorophenylhydrazone induced mitophagy only in mammalian but not yeast cells [23]. Also mitochondrial damage caused by promoter shutoff of Mdm38, a mitochondrial inner membrane protein involved in respiratory chain biogenesis and K^+ homeostasis, induced only diminutive levels of mitophagy [13,24,27,41]. But during growth on non-fermentable carbon sources enhanced vacuolar breakdown of mitochondria was observed in *yme1*Δ cells [42]. Yme1 is an AAA+ ATPase at the mitochondrial inner membrane, with a metallopeptidase domain exposed to the intermembrane space. It is conserved in humans and degrades misfolded or nonassembled proteins [43]. Upon prolonged cultivation in lactate medium *yme1*Δ cells indeed showed a moderately increased mitophagy rate compared with wild-type cells (Fig. 1C). In *yme1*Δ *atg32*Δ double knockout cells mitophagy was blocked, showing the universal nature of Atg32 as a receptor also for damaged mitochondria (not shown). Consistent with the role of Atg33 in post-log-phase mitophagy *yme1*Δ *atg33*Δ cells showed a reduced but not blocked mitophagy (not shown).

Genetic requirements of selective mitophagy induced by rapamycin

To address how mitochondrial turnover was integrated into general autophagic signaling pathways, we compared our findings with rapamycin-induced mitophagy. Therefore, we quantified the GFP signal intensities of wild-type cells expressing mito-GFP under different conditions. The 72 h value of post-log-phase mitophagy was set to 100% (Fig. 2A). Cells at the 48 h time point of post-log-phase mitophagy showed a mitophagy rate of 60%, comparable to cells after 6 h treatment with rapamycin. As the requirement of non-core autophagic proteins for rapamycin-induced mitophagy has remained enigmatic, we analysed a selected set of mutants under these conditions and found that Atg18, Atg11, Atg17, Atg29, Atg31 and Atg32 were required (Fig. 2B,C). Atg11 acts as a scaffold at the PAS during selective subtypes of autophagy, while the ternary complex of Atg17, Atg29 and Atg31 is needed for normal autophagosome biogenesis [1]. In *atg33*Δ cells rapamycin-induced mitophagy was significantly reduced but not blocked (Fig. 2B). The mitochondrial protein phosphatase homologue Aup1 has been implicated in post-log-phase mitophagy; however, its absence did not significantly affect mitophagy upon rapamycin induction (Fig. 2C) [29,44]. Also, lack of Uth1 had no significant effect on mitophagy (Fig. 2B). Using breakdown of Pgk1-GFP we followed unselective macroautophagy after rapamycin induction and detected no significant reduction in *uth1*Δ cells (not shown). Stimulation of the rapamycin-induced mitophagy rate in cells lacking Yme1 was comparable to the effect seen on post-log-phase mitophagy (Figs 2D and 1C). Again lack of Atg32 blocked rapamycin-induced mitophagy in *yme1*Δ cells, while *yme1*Δ *atg33*Δ cells only showed a reduced mitophagy rate (not shown).

To follow mitophagy by microscopy in an alternative approach, we used *pep4*Δ cells expressing mito-GFP. Due to their defect in vacuolar proteolysis, these cells accumulate autophagic bodies in the vacuole. Upon induction of mitophagy with rapamycin a significant number of mito-GFP-positive autophagic bodies could be visualized within the vacuole (Fig. 3A). In our genetic background vacuoles are easily recognized in Nomarski optics, but we also included vacuolar membrane staining with *N*-(3-triethylammoniumpropyl)-4-(*p*-diethylaminophenylhexatrienyl) pyridinium dibromide (FM4-64). Due to their autophagic defect Atg8 accumulates in *atg1*Δ cells at the PAS [45]. We grew *atg1*Δ cells expressing RFP-Atg8 and mito-GFP for 1 day in lactate medium and then added rapamycin or mock treated the cells with dimethylsulfoxide (DMSO). Also the mock treated cells showed an increased PAS rate but, as expected, treatment with rapamycin resulted in a more significant increase of cells exhibiting a PAS (Fig. 3C). To assess the morphology of the mitochondrial network, we took images of about 30 focal planes per cell (*z*-stack) and deconvoluted the images to correct for distortion. Since tubular structures in a single focal plane often appear as dots, the images of the *z*-stacks were then evaluated individually and scored in a scale ranging from 1 (no fragments) to 5 (highly fragmented) (Fig. 3B,D). As shown in Fig. 3D, rapamycin increased mitochondrial fragmentation.

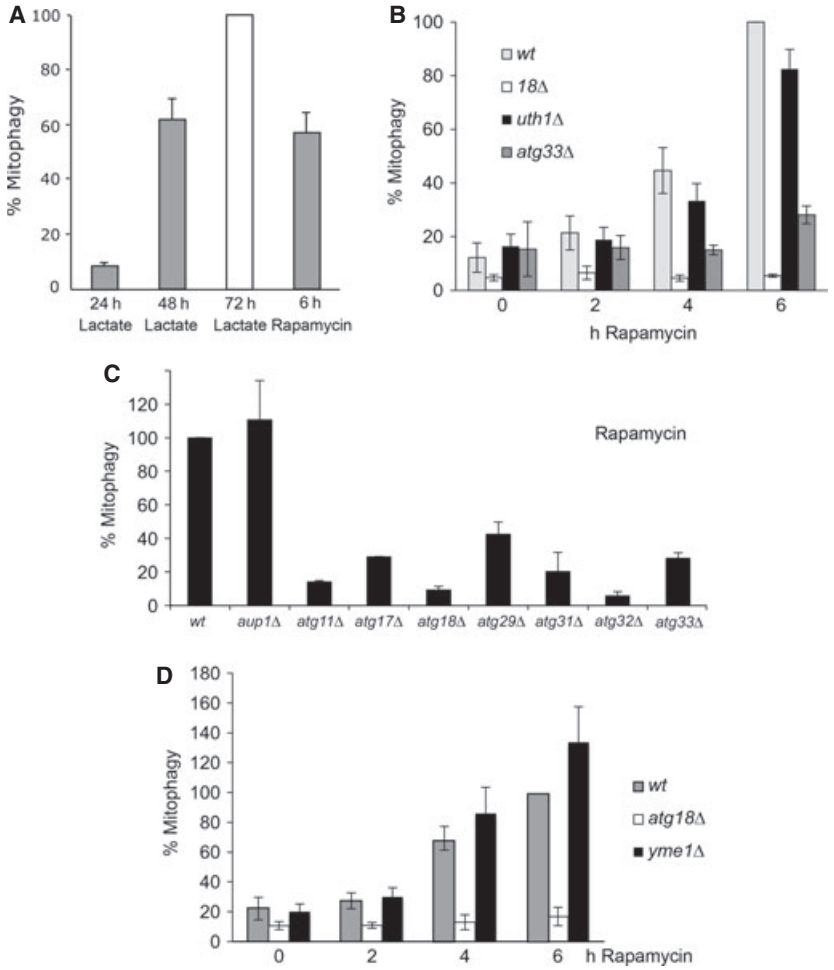

Fig. 2. Rapamycin-induced mitophagy. (A) Comparison of the mitophagy rate in wild-type cells expressing mito-GFP (mt-GFP) under the indicated conditions of mitophagy induction. Signal intensities of GFP were quantified and calculated. The value of lactate-grown cells after 72 h was set to 100%. Standard error of the mean is calculated from at least three experiments. (B) The mitophagy rate was determined as in Fig. 1. Strains of the BY4742 background were grown in selection medium with 2% lactate. After addition of 0.2 $\mu g \cdot mL^{-1}$ rapamycin, samples were taken at 0, 2, 4 and 6 h and treated as described in Experimental procedures. The value of wild-type (WT) cells treated for 6 h was set to 100%. Standard error of the mean is calculated from at least three independent experiments. (C) Mitophagy rate of the indicated deletion strains was determined after 6 h rapamycin treatment. (D) The mitophagy rate of *yme1*Δ cells was measured as in (B) after rapamycin treatment. Standard error of the mean is calculated from at least three experiments.

Uth1 is a mitochondrial inner membrane protein

A previous study suggested that Uth1 is located at the mitochondrial outer membrane and in line with this localization a role of Uth1 for selective mitophagy was suggested [28,34,38]. Since our experiments did not support an essential role of Uth1 during mitophagy, we re-evaluated both the mitochondrial import and the localization of Uth1.

Resistance of *uth1*Δ cells against rapamycin has been reported. Since this might affect autophagy induction, we analyzed the growth of *uth1*Δ cells on plates containing rapamycin. In our hands no resistance of *uth1*Δ cells to rapamycin was found (Fig. 4B); *fpr1*Δ cells served as a control for rapamycin resistance [46]. Moreover, lack of Uth1 did not significantly affect the expression level of several mitochondrial marker proteins (Fig. 4G).

Two studies suggested a Uth1 translation start that is localized 255 nucleotides downstream of an in-frame start codon (Fig. 4A) [47,48]. Interestingly, a proteomic approach to identify the N-termini of all mitochondrial proteins did not reveal N-terminal Uth1 peptides [49] (Fig. 4A). This finding could be explained if the corresponding portion of the protein is not represented in the protein databases used for protein identification. We therefore hypothesized that Uth1 translation starts in fact at the first of the two proposed start codons and that this segment of the protein would not be represented in databases. To assess import and proteolytic processing of Uth1, we used a rabbit reticulocyte lysate to *in vitro* translate and radiolabel full-length Uth1, starting from the first start codon. Remarkably, Uth1 was efficiently imported into isolated mitochondria (Fig. 4C). Surprisingly, Uth1 apparently was processed to a faster migrating form in a membrane-potential-dependent manner, which became resistant to protease added to mitochondria. This finding suggested that Uth1 was transported across the inner mitochondrial membrane [50]. We thus analyzed the localization of the imported Uth1 in detail. Again, after import Uth1 was processed in a membrane-potential-dependent manner and remained

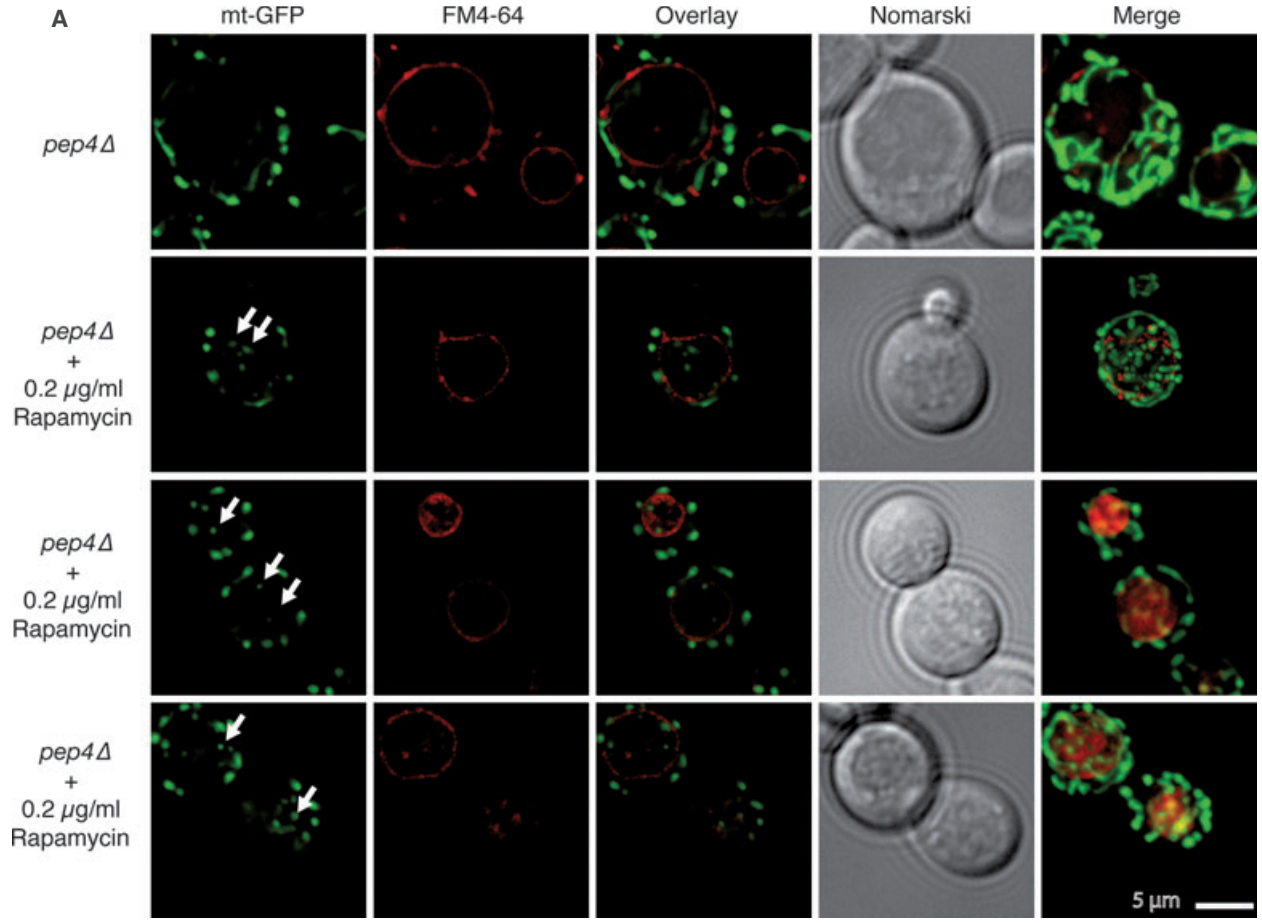

Fig. 3. Morphological analysis of mitochondria under mitophagy-inducing conditions. (A) After rapamycin treatment autophagic bodies containing mitochondria appear in the vacuole of *pep4*Δ cells. *pep4*Δ cells were treated with 0.2 $\mu g \cdot mL^{-1}$ rapamycin or mock-treated with DMSO. The vacuolar membrane was stained with FM4-64. White arrows indicate autophagic bodies with mitochondrial cargo. Overlay was made from a single plane; merge pictures were generated by merging different focal plane images into a single image (*z*-stack quick projection). (B) Monitoring the mitochondrial morphology upon onset of mitophagy. *atg1*Δ cells expressing mito-GFP (mt-GFP) and the PAS marker RFP-Atg8 were grown to stationary phase in selection medium with 2% lactate, and then mitophagy was induced for 5 h by treatment with 0.2 $\mu g \cdot mL^{-1}$ rapamycin. As a control, cells were treated with an equal amount of DMSO or examined unaffected. Vacuoles were stained with CMAC. (C) *atg1*Δ cells expressing GFP-Atg8 under the same conditions as in (B) were used to determine the PAS rate. The results are from four individual counts. (D) Evaluation of mitochondrial fragmentation. *atg1*Δ cells expressing mito-GFP were treated as described in (A). Different focal planes were evaluated and mitochondrial fragmentation was scored in a scale ranging from 1 (no fragments) up to 5 (highly fragmented). The results are from four individual counts.

protease resistant in mitochondria. However, when the outer mitochondrial membrane was permeabilized by osmotic swelling or sonication, Uth1 became accessible to protease treatment (Fig. 4D). Thus, Uth1 behaved similarly to the mitochondrial inner membrane proteins Tim23 and Tim21. This finding further supported that Uth1 localized to the inner mitochondrial membrane and was exposed to the intermembrane space. Next, we tagged Uth1 with a C-terminal FLAG-tag by chromosomal integration and isolated mitochondria from this strain. During our analyses we found that large C-terminal tags, such as GFP, lead to mislocalization of Uth1, probably due to defective transport of the protein across the outer mitochondrial membrane. Again permeabilization of the outer mitochondrial membrane by osmotic swelling or sonication led to protease accessibility of Uth1-FLAG, confirming localization of Uth1 to the inner mitochondrial membrane (Fig. 4E). To exclude differences between tagged and untagged Uth1, we synthesized radiolabeled $Uth1^{FLAG}$ in a reticulocyte lysate. After import $Uth1^{FLAG}$ was processed to a mature form in mitochondria (Fig. 4F). For comparison, we detected $Uth1^{FLAG}$ in mitochondria by western blotting. As expected, $Uth1^{FLAG}$ migrated mainly as a single band of similar size to the imported mature $Uth1^{FLAG}$

B

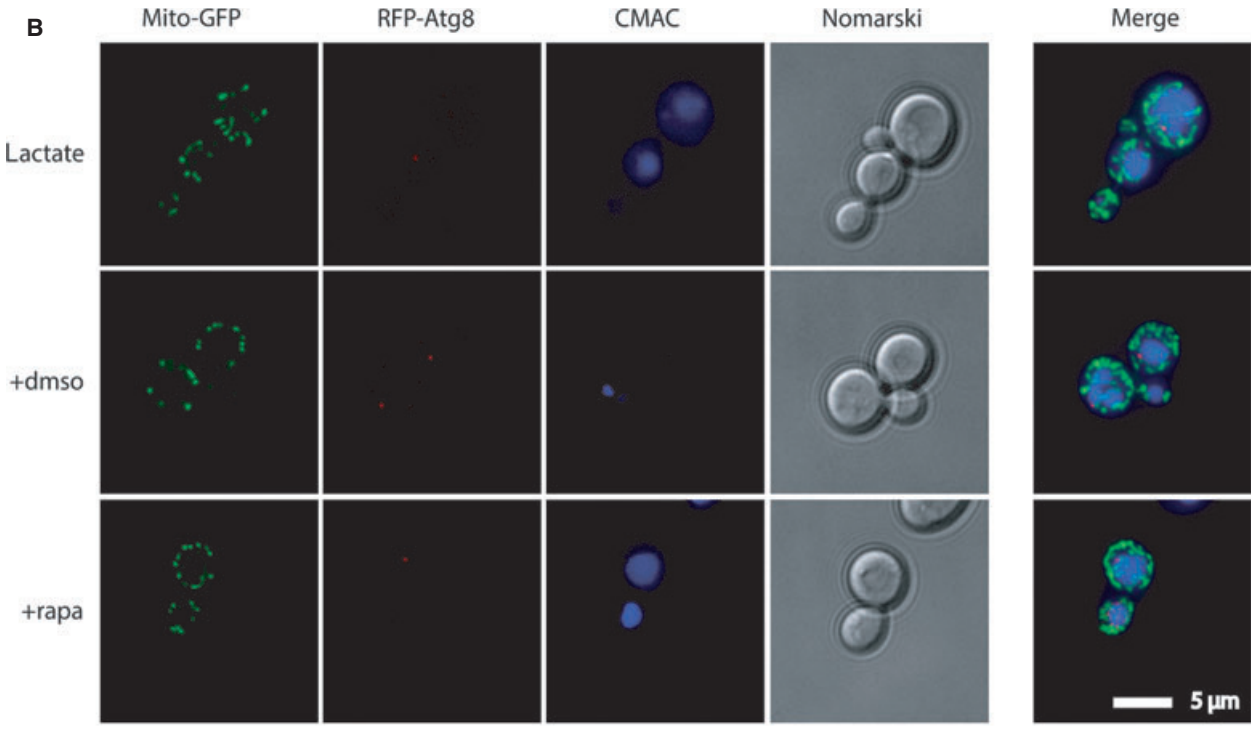

C

	No PAS	PAS
Untreated	50 +/−2 %	50 +/−2 %
DMSO	29 +/−3 %	71 +/−3 %
Rapamycin	14 +/−3 %	86 +/−3 %

D

Fragmentation group	1	2	3	4	5
Untreated	28 +/− 7,2%	**46 +/− 2,6%**	23 +/− 5,2%	2 +/− 0,6%	0 +/− 0,5%
DMSO	2 +/− 1,5%	**44 +/− 5,4%**	42 +/− 5,4%	7 +/− 3,2%	5 +/− 5,7%
Rapamycin	3 +/− 3,0%	21 +/− 3,8%	**48 +/−0,7%**	25 +/− 4,7%	2 +/− 0,4%

Fig. 3. (Continued).

(Fig. 4F). Upon long exposure, a faint band that migrated slightly above the mature $Uth1^{FLAG}$ was detectable that most probably represents a fraction of the protein in the unprocessed state. In summary, in contrast to previous findings our analyses reveal that Uth1 is a mitochondrial inner membrane protein. Treatment with 0.4 M KCl released Uth1 from mitochondrial membranes (not shown); we thus expect that Uth1 is peripherally associated with the inner mitochondrial membrane.

Discussion

Mitophagy of superfluous mitochondria

Previous studies identified a set of proteins required for selective mitophagy but not for unselective macroautophagy. These studies used different conditions for the induction of mitophagy and determined the mitophagy rate with divergent marker proteins. It is thus reasonable that the requirement of mitophagy-specific

components, especially those of Uth1, is still under debate. To compare the extent of mitophagy induction under different conditions and to dissect their genetic requirement, we monitored mitophagy in wild-type and cells lacking Atg32, Atg33 or Uth1. We observed the strongest mitophagy induction after cultivation of the cells for 72 h in lactate medium (post-log-phase mitophagy). But also addition of the TOR kinase inhibitor rapamycin for only 6 h efficiently stimulated mitophagy (Fig. 2A). Atg32 has been identified as the mitochondrial cargo receptor for post-log-phase and starvation-induced (SD-(N)) mitophagy [24,25]. In agreement, we found that Atg32 is also essential for rapamycin-induced mitophagy. Uth1 was not essential for post-log-phase or for rapamycin-induced mitophagy (Figs 1A,B and 2B). Atg33 was detected as an essential component for post-log-phase mitophagy, while it only partially affected SD-(N)-induced mitophagy [21]. We observed a reduced but not blocked rapamycin-induced and post-log-phase mitophagy in *atg33*Δ cells (Figs 1, 2). These conditions for mitophagy induction are well known to trigger robust bulk macroautophagy. Accordingly, we measured concomitant stimulation of unselective macroautophagy with induction of selective mitophagy. *atg32*Δ, *atg33*Δ or *uth1*Δ cells showed no significant inhibition of macroautophagy (not shown).

Mitochondrial damage induces selective mitophagy

Mitochondrial damage implies a great risk for the cell, demanding a tight quality control system. Mitophagy of damaged mitochondria is poorly characterized in *S. cerevisiae*. Over a decade ago, it was observed that lack of the mitochondrial ATP-dependent metalloproteinase Yme1 leads to enhanced vacuolar mitochondrial turnover [42]. We therefore analyzed mitophagy of damaged mitochondria with *yme1*Δ cells. Compared with wild-type cells *yme1*Δ cells showed a slightly enhanced mitophagy rate during prolonged cultivation in lactate medium (Fig. 1C). Unfortunately, these conditions also led to the gradual onset of post-log-phase mitophagy. This makes it difficult to separate the removal of superfluous or aged mitochondria during post-log-phase mitophagy from those damaged by the lack of Yme1. Since mitophagy was only partially affected in *yme1*Δ *atg33*Δ double mutant cells, we therefore could not determine the importance of Atg33 in mitophagy of damaged mitochondria. Nevertheless, the complete mitophagy block in *yme1*Δ *atg32*Δ cells shows that Atg32 also acts as a cargo receptor in the recognition of damaged mitochondria in *yme1*Δ cells (not shown). This is in line with the finding that the very weak mitophagy induced by promotor shutoff of Mdm38 also required Atg32 [24].

How damaged parts of the mitochondrial network are subject to mitophagy is still not fully understood. One model proposes a continuous cycle of mitochondrial fragmentation and refusion. A defect in refusion of damaged mitochondrial fragments would then open the possibility for their preferential incorporation into autophagosomes [8,51]. Indeed, escape of mitochondria from autophagic degradation by formation of an elongated tubular network during different types of starvation has been reported [20]. Our microscopic analyses of the mitochondrial network after addition of rapamycin showed enhanced mitochondrial fragmentation.

Uth1 is an inner mitochondrial membrane protein dispensable for mitophagy

Since our studies did not support an essential role of Uth1 for mitophagy, we analyzed the mitochondrial localization of Uth1. A previous study suggested localization of Uth1 at the mitochondrial outer membrane [34].

Based on the presence of an in-frame start codon 255 nucleotides upstream of the proposed ATG in *UTH1*, we speculated that translation could start at this position. Therefore, we cloned the longer version of *UTH1* (Fig. 4A). Indeed, our *in vitro* import assay showed a time-dependent maturation of Uth1 after mitochondrial import. Interestingly, the mature form of Uth1 accumulated in a membrane-potential-dependent manner and was protected against protease treatment (Fig. 4C,D). We confirmed this by determining the steady state localization of FLAG-tagged Uth1 (Fig. 4E). In contrast to the published data, our results indicate that Uth1 is a mitochondrial inner membrane protein. Since incubation in 0.4 M KCl released Uth1 from mitochondrial membranes (not shown) we conclude that it is peripherally associated with the inner membrane. Thus, localization of Uth1 and the presence of an N-terminal pre-sequence that drives the protein to the inner membrane suggest that it follows a similar transport and sorting mechanism to peripheral inner membrane proteins such as cytochrome b_2 [50,52]. This argues against a role of Uth1 as a cargo receptor protein for mitophagy. We further re-evaluated the reported rapamycin resistance but were unable to reproduce this (Fig. 4B). Our results do not support a role of Uth1 as a cargo receptor during mitophagy but point to a general role of Atg32 as a mitochondrial cargo receptor for all types of mitophagy.

A

```
MCFLLETSAS PRSKLSKDFK PQFTLLSSVT KKKKKKVRPH NFQCIHSLNF VYFLFIHSFL  60
FEYNQLLVLP LNKNLPSLNF SRNSSMKLSA LLALSASTAV LAAPAVHHSD NHHHNDKRAV 120
VTVTQYVNAD GAVVIPAATT ATSAAADGKV ESVAAATTTL SSTAAAATTS AAASSSSSSS 180
SSSSSSSVG SGDFEDGTIS CSDFPSGQGA VSLDWLGLGG WASIMDMNGN TATSCQDGYY 240
CSYACSPGYA KTQWPSEQPS DGRSVGGLYC KNGKLYRSNT DTNSLCVEGQ GSAQAVNKVS 300
GSIAICGTDY PGSENMVVPT VVGAGSSQPI NVIKEDSYYQ WQGKKTSAQY YVNNAGVSVE 360
DGCIWGTEGS GVGNWAPVVL GAGYTDGITY LSIIPNPNNK EAPNFNIKIV ATDGSTVNGA 420
CSYENGVYSG SGSDGCTVSV TSGSANFVFY
```

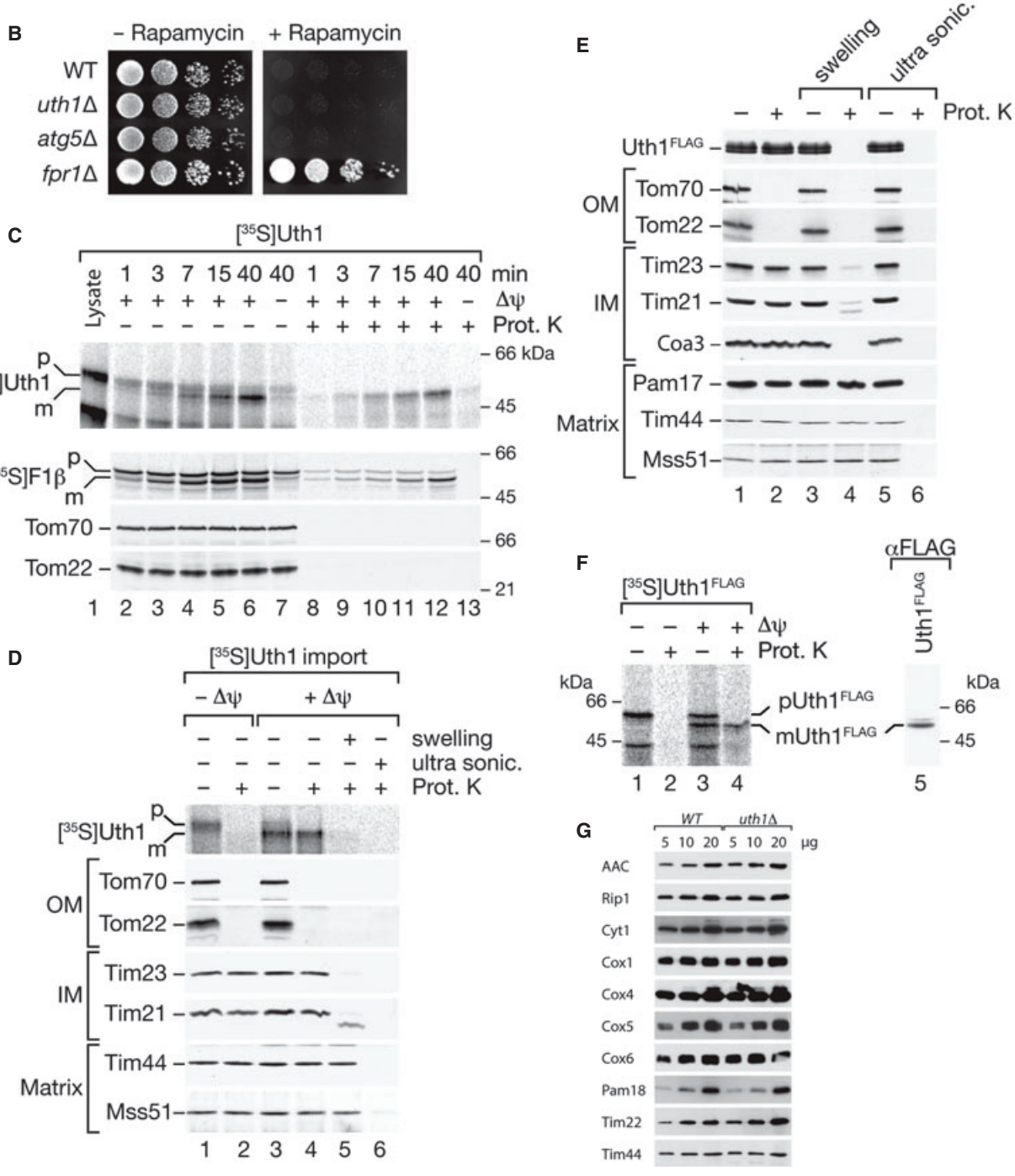

Fig. 4. Mitochondrial localization of Uth1. (A) Amino acid sequence of Uth1: potential start methionines, grey boxes; predicted transmembrane span, underlined. (B) Serial dilutions of indicated yeast strains (BY4742) were spotted on YPD plates containing 0.2 μg·mL^{-1} rapamycin where indicated. Plates were incubated for 3 days at 30 °C. (C) *In vitro* import of ^{35}S-labeled Uth1 into isolated yeast mitochondria in the presence or absence of a membrane potential ($\Delta\psi$). Where indicated samples were treated with proteinase K (Prot. K). p, precursor; m, mature. (*In vitro* translation of *UTH1* gave rise to two products; the smaller probably represents an internal translation initiation product (lane 1) which is not imported into mitochondria; see below.) *In vitro* import of F1β as a control for inner membrane translocation. From the same experiment, Tom22 and Tom70 were detected by western blotting. (D) Radiolabeled Uth1 was imported into mitochondria as in (C). After import mitochondria were subjected to osmotic treatment, sonication or left untreated. Where indicated, samples were subjected to proteinase K digestion. OM, outer membrane; IM, inner membrane. (E) Isolated yeast mitochondria from Uth1^{FLAG} expressing cells were left untreated or subjected to osmotic swelling or sonication and treated with proteinase K as indicated. Samples were analyzed by SDS/PAGE and western blotting. Uth1^{FLAG} signals were compared with marker proteins of the outer membrane (OM), inner membrane (IM) and matrix. (F) ^{35}S-labeled Uth1^{FLAG} was imported into mitochondria as in (C). For comparison mitochondria containing Uth1^{FLAG} were decorated with anti-FLAG antibodies. (G) The expression level of different marker proteins was analyzed in western blots from mitochondria isolated from wild-type and *uth1*Δ cells.

Experimental procedures

Strains

Deletion strains were of the BY4742 background (Euroscarf, Frankfurt, Germany) or derived from WCG4α Matα *ura3 his3-11,15 leu2-3,112* [53]. Further chromosomal deletions in the WCG4α background (*yme1*Δ::kan, *atg32*Δ::nat, *atg33*Δ::nat, *yme1*Δ::kan *atg32*Δ::nat and *yme1*Δ::kan *atg33*Δ::nat) and BY4742 background (*aup1*Δ::nat) were generated by chromosomal integration of a PCR fragment consisting of KANMX6 [54] or NATMX4 [55]. The fragments were constructed with plasmid pFA6a-kanMX6 or pFA6-natNT2 and primers Yme1-kan forward, TAT AAT ACA TTG TGG ATA GAA CGA AAA CAG AGA CGT GAT AGc agc tga agc ttc gta cgc; Yme1-kan reverse, GT CTT GAG GTA GGT TCC TTC ATA CGT TTA ACT TCT TAG AAg cat agg cca cta gtg gatc; atg32_ko_frw, CTT ATC AGT TGT GAC TTC TCT T A TCG ATA AGC AAT ATT GAA GTC CTA ATC ACC GTA CGC TGC AGG TCG AC; atg32_ko_rev, GCT TCT ATG TAA TTA AGG AAA GGA ACC AAA CGG GGA ATA TAG ATA CGC AGT GAT CGA TGA ATT CGA GCT CG; atg33_ko_frw, CAA CGT TCT TAG CCA AAT TCG CTT ATC ACT TAC TAC TTC ACG ATA TAC AGA AGC GTA CGC TGC AGG TCG AC; atg33_ko_rev, TTA CTA CAC ACT TTA TTT TTG GAG AGA GAG AGG AGC CGA GGT TCA GGC AGC ATC GAT GAA TTC GAG CTC G; aup1_ko_frw, CAA TAA CAG GCT GCA ATC GGG GCA ATT AAG CAT CAG AAG AGG GGC GTA CGC TGC AGG TCG AC; and aup1_ko_rev, CCC AGG GGG GTG TTT AGT TTA ATT TTG TTT CGT TAG ATT GTG CAA TCG ATG AAT TCG AGC TCG. Transformants were selected on plates containing 200 μg·L^{-1} kanamycin (Roth, Karlsruhe, Germany) or 100 μg·L^{-1} nourseothricin (Werner Bioagents, Jena, Germany). Yeast strains for isolation of mitochondria were of YPH499 background (*MAT*a *ade2-101 his3-Δ200 leu2-Δ1 lys2-801 trp1-Δ63 ura3-52*) [56]. The yeast strain yRR31 (Uth1^{FLAG}) (*MAT*a *ade2-101 his3-Δ200 leu2-Δ1 ura3-52 trp1-Δ63 lys2-801 uth1::UTH1^{FLAG}-His3MX6*), expressing a FLAG-tag, fused to the C-terminus of Uth1 was generated by chromosomal integration of a FLAG cassette downstream of the *UTH1* open reading frame in the strain YPH499.

Plasmids

To monitor mitophagy the plasmid mito-GFP was constructed by the insertion of a Su9-DHFR fragment into the vector pUG35 (a centromeric *URA3* vector for generation of carboxyterminal GFP fusions under control of the *MET25* promoter). The fragment was generated with the template Su9-DHFR (Su9, subunit of the *N. crassa* F_1F_0 ATPase; DHFR, dihydrofolate reductase) and the primers Su9 forward tct aga gga tcc atg gcc tcc act cgt gtc ctc g and Su9 reverse gtc gac aag ctt gtc ttt ctt ctc gta gac ttc aaa c and treated with *Bam*HI and *Hin*dIII.

Monitoring mitophagy and macroautophagy in western blots

To monitor macroautophagy the plasmid Pgk1-GFP [40] and to monitor mitophagy the plasmid mito-GFP were used. Cells expressing the marker protein were cultured to stationary phase using standard medium for precultures as described in [57]. For mitochondrial proliferation CM selection medium (0.67% yeast nitrogen base without amino acids (BD Difco, Heidelberg, Germany), 0.2% Dropout-Mix, pH 5.5) lacking methionine and supplemented with 2% lactate as sole carbon source was used for main cultures. Stationary grown cells were cultured up to 3 days or treated with 0.2 μg·mL^{-1} rapamycin to induce autophagy. Samples were taken at defined time points, alkaline lysed and precipitated with trichloroacetic acid. Extracts were separated by SDS/PAGE (containing 6 M urea) followed by western blotting using a GFP antibody (Roche, Mannheim, Germany) and a secondary antibody coupled to peroxidase. Detection was performed by use of an enhanced chemiluminescence

detection kit (Amersham, Braunschweig, Germany) and an LAS3000 imaging system. For quantification of the GFP signal the AIDA software package was used. Error bars are calculated from at least three independent experiments. The wild type was set to 100%.

Microscopy

A DeltaVision Spectris (Applied Precision, Issaquah, WA, USA) fluorescence microscope equipped with a 100 × objective and FITC, TRITC and DAPI filter set (excitation wavelengths of 340–380, 465–495 and 540–580 nm and emission wavelengths of 435–485, 515–555 and 572–605 nm, respectively) was used. Vacuolar staining was performed using 32 μM FM4-64 (Invitrogen, Darmstadt, Germany) for 30 min or 100 nM 4-chloromethyl-7-aminocoumarin (CMAC) (Invitrogen) for 10 min. 5 μL of liquid cultured cells were used. Pictures were taken and deconvoluted using WORX (Applied Precision LLC) software and processed using Adobe Photoshop and Illustrator software.

Determination of PAS rate

*atg1*Δ cells expressing the PAS marker GFP-Atg8 were cultured as described above and treated with DMSO, rapamycin or left unaffected and were used for microscopy. Cells presenting a PAS signal (i.e. GFP-Atg8 dots near the vacuole) were statistically evaluated.

Mitochondrial fragmentation

*atg1*Δ cells expressing mito-GFP were used for microscopy. A series of images were taken in different focal planes (*z*-stack). Mitochondrial fragmentation was scored in a scale ranging from 1 (no fragments) to 5 (highly fragmented) and the percentage of cells in each category of individual assessments was calculated. To avoid bias samples were processed by one person and evaluated by another person, without knowing the identity of the individual strains. The percentage of cells in each category was then calculated and errors determined based on four individual determinations.

Isolation of yeast mitochondria, *in vitro* import studies

Mitochondria from yeast cells (YPH499), grown at 30 °C in yeast extract-peptone-glycerol were isolated as described in [58]. For *in vitro* translation the open reading frame of *UTH1* was PCR amplified from yeast genomic DNA and a SP6 promoter was introduced with the primers UTH1FOR, GGA TTT AGG TGA CAC TAT AGA ATA CAT GTG TTT CCT TCT CGA G, and UTH1REV, GTA CTA GCA AAA GCT TAT T. Analogously, the open reading frame encoding FLAG-tagged Uth1 was PCR amplified from genomic DNA of the strain yRR31 ($Uth1^{FLAG}$) with primers UTH1FOR and oRR36 (ACA AAGCTT TGGGCCTCCATGTCGCTGG). The PCR products were *in vitro* transcribed using the mMessage mMachine SP6 system (Ambion, Invitrogen, Karlsruhe, Germany) and mRNA purified with the MEGAclear kit (Ambion). Subsequently the Uth1 precursor proteins were *in vitro* translated and ^{35}S-labeled using the Flexi Rabbit Reticulocyte-Lysate system (Promega, Mannheim, Germany). *In vitro* import of radiolabeled precursor proteins into isolated yeast mitochondria was performed as described previously [59]. Samples were analyzed by SDS/PAGE and radiolabeled proteins were detected by digital autoradiography.

For analysis of submitochondrial localization of proteins, the mitochondrial outer membrane was disrupted by osmotic swelling in 1 mM EDTA, 10 mM MOPS (pH 7.2) prior to treatment with 20 $\mu g \cdot mL^{-1}$ proteinase K for 10 min at 4 °C. Alternatively the outer and inner membrane was permeabilized by sonication in the presence of 20 $\mu g \cdot mL^{-1}$ proteinase K followed by incubation for 10 min at 4 °C.

Acknowledgements

This study was supported by the Deutsche Forschungsgemeinschaft, the Max Planck Society (PR) and the Göttingen Graduate School for Neurosciences, Biophysics, and Molecular Biosciences. For helpful discussions and technical help we thank R.P. Zahedi, A. Sickmann, C. Meisinger and S. Jakobs. The authors declare no conflict of interest.

References

1 Mizushima N, Yoshimori T & Ohsumi Y (2011) The role of Atg proteins in autophagosome formation. *Annu Rev Cell Dev Biol* **27**, 107–132.
2 Levine B, Mizushima N & Virgin HW (2011) Autophagy in immunity and inflammation. *Nature* **469**, 323–335.
3 Farré J-C, Krick R, Subramani S & Thumm M (2009) Turnover of organelles by autophagy in yeast. *Curr Opin Cell Biol* **21**, 522–530.
4 Yang Z & Klionsky DJ (2010) Eaten alive: a history of macroautophagy. *Nat Cell Biol* **12**, 814–822.
5 Okamoto K & Kondo-Okamoto N (2011) Mitochondria and autophagy: critical interplay between the two homeostats. *Biochim Biophys Acta* **1820**, 595–600.
6 Kanki T, Klionsky DJ & Okamoto K (2011) Mitochondria autophagy in yeast. *Antioxid Redox Signal* **14**, 1989–2001.
7 Wang K & Klionsky DJ (2011) Mitochondria removal by autophagy. *Autophagy* **7**, 297–300.
8 Youle RJ & Narendra DP (2011) Mechanisms of mitophagy. *Nat Rev Mol Cell Biol* **12**, 9–14.

9 Sandoval H, Thiagarajan P, Dasgupta SK, Schumacher A, Prchal JT, Chen M & Wang J (2008) Essential role for Nix in autophagic maturation of erythroid cells. *Nature* **454**, 232–235.
10 Novak I, Kirkin V, McEwan DG, Zhang J, Wild P, Rozenknop A, Rogov V, Löhr F, Popovic D, Occhipinti A *et al*. (2010) Nix is a selective autophagy receptor for mitochondrial clearance. *EMBO Rep* **11**, 45–51.
11 Schwarten M, Mohrlüder J, Ma P, Stoldt M, Thielmann Y, Stangler T, Hersch N, Hoffmann B, Merkel R & Willbold D (2009) Nix directly binds to GABARAP: a possible crosstalk between apoptosis and autophagy. *Autophagy* **5**, 690–698.
12 Nishida Y, Arakawa S, Fujitani K, Yamaguchi H, Mizuta T, Kanaseki T, Komatsu M, Otsu K, Tsujimoto Y & Shimizu S (2009) Discovery of Atg5/Atg7-independent alternative macroautophagy. *Nature* **461**, 654–658.
13 Narendra D, Tanaka A, Suen D-F & Youle RJ (2008) Parkin is recruited selectively to impaired mitochondria and promotes their autophagy. *J Cell Biol* **183**, 795–803.
14 Narendra DP, Jin SM, Tanaka A, Suen D-F, Gautier CA, Shen J, Cookson MR & Youle RJ (2010) PINK1 is selectively stabilized on impaired mitochondria to activate Parkin. *PLoS Biol* **8**, e1000298.
15 Geisler S, Holmström KM, Skujat D, Fiesel FC, Rothfuss OC, Kahle PJ & Springer W (2010) PINK1/Parkin-mediated mitophagy is dependent on VDAC1 and p62/SQSTM1. *Nat Cell Biol* **12**, 119–131.
16 Gegg ME, Cooper JM, Chau K-Y, Rojo M, Schapira AHV & Taanman J-W (2010) Mitofusin 1 and mitofusin 2 are ubiquitinated in a PINK1/parkin-dependent manner upon induction of mitophagy. *Hum Mol Genet* **19**, 4861–4870.
17 Poole AC, Thomas RE, Yu S, Vincow ES & Pallanck L (2010) The mitochondrial fusion-promoting factor mitofusin is a substrate of the PINK1/parkin pathway. *PLoS ONE* **5**, e10054.
18 Ziviani E, Tao RN & Whitworth AJ (2010) Drosophila parkin requires PINK1 for mitochondrial translocation and ubiquitinates mitofusin. *Proc Natl Acad Sci USA* **107**, 5018–5023.
19 Tanaka A, Cleland MM, Xu S, Narendra DP, Suen D-F, Karbowski M & Youle RJ (2010) Proteasome and p97 mediate mitophagy and degradation of mitofusins induced by Parkin. *J Cell Biol* **191**, 1367–1380.
20 Rambold AS, Kostelecky B, Elia N & Lippincott-Schwartz J (2011) Tubular network formation protects mitochondria from autophagosomal degradation during nutrient starvation. *Proc Natl Acad Sci U S A* **108**, 10190–10195.
21 Kanki T, Wang K, Baba M, Bartholomew CR, Lynch-Day MA, Du Z, Geng J, Mao K, Yang Z, Yen W-L *et al*. (2009) A genomic screen for yeast mutants defective in selective mitochondria autophagy. *Mol Biol Cell* **20**, 4730–4738.
22 Nowikovsky K, Reipert S, Devenish RJ & Schweyen RJ (2007) Mdm38 protein depletion causes loss of mitochondrial K^+/H^+ exchange activity, osmotic swelling and mitophagy. *Cell Death Differ* **14**, 1647–1656.
23 Mendl N, Occhipinti A, Muller M, Wild P, Dikic I & Reichert AS (2011) Mitophagy in yeast is independent of mitochondrial fission and requires the stress response gene WHI2. *J Cell Sci* **124**, 1339–1350.
24 Kanki T, Wang K, Cao Y, Baba M & Klionsky DJ (2009) Atg32 is a mitochondrial protein that confers selectivity during mitophagy. *Dev Cell* **17**, 98–109.
25 Okamoto K, Kondo-Okamoto N & Ohsumi Y (2009) Mitochondria-anchored receptor Atg32 mediates degradation of mitochondria via selective autophagy. *Dev Cell* **17**, 87–97.
26 Aoki Y, Kanki T, Hirota Y, Kurihara Y, Saigusa T, Uchiumi T & Kang D (2011) Phosphorylation of serine 114 on Atg32 mediates mitophagy. *Mol Biol Cell* **22**, 3206–3217.
27 Kanki T & Klionsky DJ (2008) Mitophagy in yeast occurs through a selective mechanism. *J Biol Chem* **283**, 32386–32393.
28 Deffieu M, Bhatia-Kissova I, Salin B, Galinier A, Manon S & Camougrand N (2009) Glutathione participates in the regulation of mitophagy in yeast. *J Biol Chem* **284**, 14828–14837.
29 Tal R, Winter G, Ecker N, Klionsky DJ & Abeliovich H (2007) Aup1p, a yeast mitochondrial protein phosphatase homolog, is required for efficient stationary phase mitophagy and cell survival. *J Biol Chem* **282**, 5617–5624.
30 Kroemer G & Levine B (2008) Autophagic cell death: the story of a misnomer. *Nat Rev Mol Cell Biol* **9**, 1004–1010.
31 Tatsuta T & Langer T (2008) Quality control of mitochondria: protection against neurodegeneration and ageing. *EMBO J* **27**, 306–314.
32 Scherz-Shouval R & Elazar Z (2011) Regulation of autophagy by ROS: physiology and pathology. *Trends Biochem Sci* **36**, 30–38.
33 Ritch JJ, Davidson SM, Sheehan JJ & Austriaco N (2010) The Saccharomyces SUN gene, UTH1, is involved in cell wall biogenesis. *FEMS Yeast Res* **10**, 168–176.
34 Velours G, Boucheron C, Manon S & Camougrand N (2002) Dual cell wall/mitochondria localization of the 'SUN' family proteins. *FEMS Microbiol Lett* **207**, 165–172.

35 Bhatia-Kiššová I & Camougrand N (2010) Mitophagy in yeast: actors and physiological roles. *FEMS Yeast Res* **10**, 1023–1034.
36 Bandara PD, Flattery-O'Brien JA, Grant CM & Dawes IW (1998) Involvement of the *Saccharomyces cerevisiae* UTH1 gene in the oxidative-stress response. *Curr Genet* **34**, 259–268.
37 Kissová I, Deffieu M, Manon S & Camougrand N (2004) Uth1p is involved in the autophagic degradation of mitochondria. *J Biol Chem* **279**, 39068–39074.
38 Kissová I, Salin B, Schaeffer J, Bhatia S, Manon S & Camougrand N (2007) Selective and non-selective autophagic degradation of mitochondria in yeast. *Autophagy* **3**, 329–336.
39 Kanki T, Kang D & Klionsky DJ (2009) Monitoring mitophagy in yeast: the Om45-GFP processing assay. *Autophagy* **5**, 1186–1189.
40 Welter E, Thumm M & Krick R (2010) Quantification of nonselective bulk autophagy in *S. cerevisiae* using Pgk1-GFP. *Autophagy* **6**, 794–797.
41 Lupo D, Vollmer C, Deckers M, Mick DU, Tews I, Sinning I & Rehling P (2011) Mdm38 is a 14-3-3-like receptor and associates with the protein synthesis machinery at the inner mitochondrial membrane. *Traffic* **12**, 1457–1466.
42 Campbell CL & Thorsness PE (1998) Escape of mitochondrial DNA to the nucleus in yme1 yeast is mediated by vacuolar-dependent turnover of abnormal mitochondrial compartments. *J Cell Sci* **111** (Pt 16), 2455–2464.
43 Graef M, Seewald G & Langer T (2007) Substrate recognition by AAA+ ATPases: distinct substrate binding modes in ATP-dependent protease Yme1 of the mitochondrial intermembrane space. *Mol Cell Biol* **27**, 2476–2485.
44 Journo D, Mor A & Abeliovich H (2009) Aup1-mediated regulation of Rtg3 during mitophagy. *J Biol Chem* **284**, 35885–35895.
45 Suzuki K, Kubota Y, Sekito T & Ohsumi Y (2007) Hierarchy of Atg proteins in pre-autophagosomal structure organization. *Genes Cells* **12**, 209–218.
46 Heitman J, Movva NR & Hall MN (1991) Targets for cell cycle arrest by the immunosuppressant rapamycin in yeast. *Science* **253**, 905–909.
47 Kellis M, Patterson N, Endrizzi M, Birren B & Lander ES (2003) Sequencing and comparison of yeast species to identify genes and regulatory elements. *Nature* **423**, 241–254.
48 Zhang Z & Dietrich FS (2005) Mapping of transcription start sites in *Saccharomyces cerevisiae* using 5′ SAGE. *Nucleic Acids Res* **33**, 2838–2851.
49 Vögtle F-N, Wortelkamp S, Zahedi RP, Becker D, Leidhold C, Gevaert K, Kellermann J, Voos W, Sickmann A, Pfanner N *et al.* (2009) Global analysis of the mitochondrial N-proteome identifies a processing peptidase critical for protein stability. *Cell* **139**, 428–439.
50 van der Laan M, Rissler M & Rehling P (2006) Mitochondrial preprotein translocases as dynamic molecular machines. *FEMS Yeast Res* **6**, 849–861.
51 Twig G, Hyde B & Shirihai OS (2008) Mitochondrial fusion, fission and autophagy as a quality control axis: the bioenergetic view. *Biochim Biophys Acta* **1777**, 1092–1097.
52 Herrmann JM & Hell K (2005) Chopped, trapped or tacked – protein translocation into the IMS of mitochondria. *Trends Biochem Sci* **30**, 205–211.
53 Thumm M, Egner R, Koch B, Schlumpberger M, Straub M, Veenhuis M & Wolf DH (1994) Isolation of autophagocytosis mutants of *Saccharomyces cerevisiae*. *FEBS Lett* **349**, 275–280.
54 Longtine M, McKenzie A, Demarini D, Shah N, Wach A, Brachat A, Philippsen P & Pringle J (1998) Additional modules for versatile and economical PCR-based gene deletion and modification in *Saccharomyces cerevisiae*. *Yeast* **14**, 953–961.
55 Knop M, Siegers K, Pereira G, Zachariae W, Winsor B, Nasmyth K & Schiebel E (1999) Epitope tagging of yeast genes using a PCR-based strategy: more tags and improved practical routines. *Yeast* **15**, 963–972.
56 Sikorski R & Hieter P (1989) A system of shuttle vectors and yeast host strains designed for efficient manipulation of DNA in *Saccharomyces cerevisiae*. *Genetics* **122**, 19–27.
57 Ausubel F, Brent R, Kingston R & Moore D (1987) Current Protocols in Molecular Biology. Greene Publishing Associates, New York, NY.
58 Meisinger C, Pfanner N & Truscott KN (2006) Isolation of yeast mitochondria. *Methods Mol Biol* **313**, 33–39.
59 Wiedemann N, Pfanner N & Rehling P (2006) Import of precursor proteins into isolated yeast mitochondria. *Methods Mol Biol* **313**, 373–383.